$$\cos\phi = \frac{\sqrt{3}\cos\psi + \cos\theta}{\sqrt{2}\sin\theta} \tag{13}$$

where, as ϕ varies from 0–60°, ψ varies from 0–45°. The plots of σ on Γ versus ψ are given in Fig. 3. To obtain $\sigma(r, \theta, \phi)$ at arbitrary points of the squares, choose any ψ, compute θ and ϕ from (12) and (13), substitute into (11), and multiply by $a_0 \varepsilon r^{\alpha-1}$. The concentration of charge at the apex of the corner is exhibited by the factor $r^{\alpha-1}$.

Observe in that Fig. 3, σ varies from a low value at $\psi = 45°$, which represents a point along the diagonal of the square, to higher values as ψ decreases, i.e., as the point approaches an edge of the square, and then tapers off as ψ reaches 0, i.e., as the point reaches that edge. The initial increase is expected, but the tapering off is not because charge should concentrate more strongly near the edges of the conductor as well as at its apex. We feel that this tapering off is consequence of our truncation of (2) at low value of N. Indeed, note that, as compared to the case when $N = 2$, for $N = 3$ σ is smaller toward the center of the square, rises more sharply as the edge is approached, and then tapers off less. We expect that this improvement will continue as N is increased beyond $N = 3$. Moreover, we also feel that this tapering off does not much matter because the areas under both curves of Fig. 3 are not much different. It is the increase in this area multiplied by $r^{1-\alpha}$ which primarily determines the field singularity at the apex. Our expectation that our formula (1), which is obtained for $N = 3$, will not change by much had we chosen $N = 4$ is reinforced by the fact that the numerical coefficient in (1) changes by only seven tenths of one percent when going from $N = 2$ to $N = 3$.

The final step of our derivation is the integration of (11) over all three squares to obtain the total charge Q on all three shaded areas of Fig. 1. The result is our formula (1).

IV. Two Examples

In order to ascertain how much corner and edge field singularities affect a typical capacitance computation and also to compare our numerical results with other results in the literature, we computed capacitances for two conductor configurations over a ground plane.

Example A: Consider the single conductor, shown in Fig. 4, of 5 m length, 5 m width, 1 m thickness, 2 m above a perfectly conducting plane, and imbedded in a medium of unit dielectric permittivity ($\varepsilon = 1$). If we ignore the singularities of the electrical field at corners and edges, but allow incremental areas of the finite-difference method to extend beyond edges, the value of capacitance C is 49.10 F. If incremental areas extending beyond edges are deleted, the result is 34.82 F. If we consider edge singularities only and extended areas are deleted, the result is 39.79. On the other hand, if we consider both factors, i.e., in the most accurate case where all singularities are considered but extended areas are deleted, we get C equal to 41.64 F when $N = 2$ and 41.61 F when $N = 3$. These results can be compared to the capacitance value given by Ruehli and Brennan in [3] by interpolating in their Fig. 2 where they use the sharp edge and corner model. Their result is 42.5 F. These capacitances are listed in Table I.

Example B: Consider now a right-angle bend 2 m above a perfectly conducting plane with $\varepsilon = 1$ for the medium. Its dimensions are shown in Fig. 5. If we do not consider the singularities of the electrical field at corners and edges but allow overextending incremental areas, the value of capacitance C is 106.06 F. If overextending areas are deleted, the result is 73.93 F. If we consider edge singularities only and extended areas are deleted, the result is 79.48. On the other hand, if we correct both factors, we get C is 81.22 F for $N = 2$ and 81.19 F for $N = 3$. These results can be compared to the capacitance value given by Ruehli and Brennan in [4] by interpolating in their Fig. 9; their value is 101.2 F. These capacitances are listed in Table II.

References

[1] A. E. Beagles and J. R. Whiteman, "General conical singularities in three-dimensional Poisson problems," *Math. Meth. Appl. Sci.*, vol. 11, pp. 215–235, 1989.

[2] J. W. Duncan, "The accuracy of finite-difference solutions of Laplace's equation," *IEEE Trans. Microwave Theory Tech.*, vol. MTT-15, pp. 575–582, 1967.

[3] A. E. Ruehli and P. A. Brennan, "Accurate metallization capacitances for integrated circuits and packages," *IEEE J. Solid-State Circuits*, vol. SSC-8, pp. 289–290, 1973.

[4] ——, "Capacitance modals for integrated circuit metallization wires," *IEEE J. Solid-State Circuits*, vol. SSC-10, pp. 530–536, 1975.

[5] A. H. Zemanian, "A finite-difference procedure for the exterior problem inherent in capacitance computations for VLSI interconnections," *IEEE Trans. Electron Devices*, vol. 35, pp. 985–992, 1988.

[6] A. H. Zemanian, P. R. Tewarson, C. P. Ju, and J. F. Jen, "Three-dimensional capacitance computations for VLSI/ULSI interconnections," *IEEE Trans. Computer-Aided Design*, vol. 8, pp. 1319–1326, 1989.

[7] Y. Zhang, *Three-Dimensional Corner Singularities in VLSI Capacitance Estimation*, Ph.D. dissertation, University at Stony Brook, Stony Brook, NY, 1995.

Computation of Equivalent Circuits of CPW Discontinuities Using Quasi-Static Spectral Domain Method

D. Mirshekar-Syahkal

***Abstract*— An efficient and simple computer technique based on the quasistatic approximation for the determination of the component values of the equivalent circuits of a broad-class of coplanar waveguide (CPW) discontinuities is introduced. The technique does not depend on the extraction of the component values from the scattering parameters. It uses the spectral domain formulation in conjunction with the method of moments. The concepts behind the method are illustrated using a complex example, the CPW T-junction. A few T-junctions are treated with the technique. Both the measurements and the full-wave electromagnetic simulation support the accuracy of the results.**

I. Introduction

For some of its advantages, the coplanar waveguide (CPW) is preferred to the microstrip line in developing monolithic microwave integrated circuits (MMIC's) on GaAs and InP. This transmission line has also found extensive applications at mm-wave and terahertz frequencies [1]. However, due to lack of powerful software, design of CPW circuits is difficult and time consuming. A comprehensive software should contain the equivalent circuits of various CPW discontinuities including bends, open and short terminations, steps, etc.

Recently, Naghed and Wolf [2], Naghed *et al.* [3], and Abdo-Tuko *et al.* [4] used the three-dimensional finite difference method to char-

Manuscript received October 17, 1995; revised February 15, 1996.

The author is with the Department of Electronic Systems Engineering, University of Essex, Colchester, Essex CO4 3SQ U.K.

Publisher Item Identifier S 0018-9480(96)03790-8.

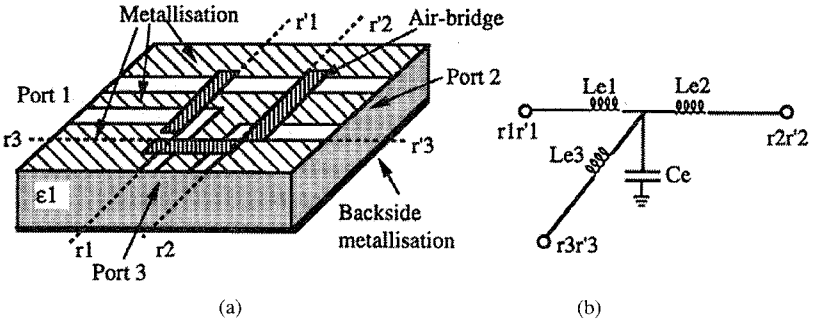

Fig. 1. (a) A CPW T-junction, and (b) the equivalent circuit of the area of the junction bounded to the reference planes.

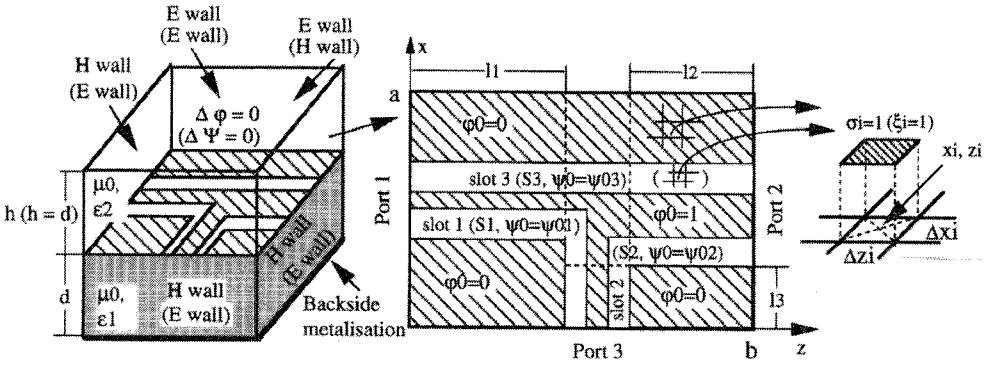

Fig. 2. (a)–(b) The electrostatic problem for the computation of the equivalent capacitance and the problem (specified within the brackets) for the calculation of equivalent inductances, and (c) the top-hat basis function for approximating the charge distribution on the metallization and the normal component of the magnetic field distribution at the slots.

acterize various CPW discontinuities under the quasistatic regime. The approach is general and can deal with complex geometries. However, for many CPW structures, such an approach may not be necessary.

This paper introduces a very efficient computer technique for the determination of the element values of equivalent circuits of a broad-class of CPW discontinuities. Its high computation efficiency follows from the pseudo-numerical nature of the technique. The technique is demonstrated by applying it to the CPW T-junction. However, it can be readily used to find the equivalent circuits of other discontinuities. The T-junction is particularly important for its use in biasing active devices as well as in matching methods employing stubs.

Since the technique is based on the assumption of the quasi-TEM wave propagation in a CPW structure, the electric and magnetic fields around the junction can be derived from electric and magnetic potentials which are the solutions of the Laplace equation. These solutions are obtained using the quasistatic spectral domain formulation in conjunction with the moment method. As will be shown later, in the application of the moment method when solving for the magnetic potential, the function chosen for the expansion is the normal component of the magnetic field at the slots and when solving for the electric potential, it is the charge distributions on the conductors. These choices reduce the number of the basis functions and hence reduce the computation effort. The expansion functions adopted here are top-hat functions which due to their simplicity offer savings in computer memory and time. For achieving an even higher computation efficiency, the discretization of the solution space can be made nonuniform and adaptive to the shape of the discontinuity. The technique is suitable for parallel processing and can be used in conjunction with wavelet basis functions. Such implementations further reduce the computation time.

Results presented include a convergence test for a symmetrical T-junction and the component values of the equivalent circuits of two other T-junctions. For the theoretical verification of the results, a full-wave electromagnetic simulator was used [5] .

II. Application of the Technique to a CPW T-Junction

A. The Equivalent Circuit

The structure of a CPW T-junction is shown in Fig. 1(a). Under the quasistatic approximation, the air-bridges may be modeled by shunt capacitors. In MMIC's, an air-bridge usually have a height much smaller than its width in which case the fringing field may be ignored and the capacitance of the air-bridge can be approximated by that of a parallel plate capacitor.

Now consider the central part of the junction bounded to reference planes $r_p r_p'$ (p =1, 2, 3), Fig. 1(a). This region is assumed to have dimensions much smaller than the wavelength, and under the quasi-TEM assumption, its field is expected to change negligibly with frequency. These assumptions allow the equivalent circuit of the region to be defined as a combination of lumped frequency independent capacitors and inductors. A good model for the equivalent circuit consists essentially of a shunt capacitor and three series inductors [3], [4], Fig. 1(b).

The concept adopted here in order to compute the values of the components in the equivalent circuit in Fig. 1(b) follows that presented in [6] for the evaluation of equivalent capacitances of microstrip open circuits and in [7] for the calculation of microstrip discontinuity inductances. It basically involves defining ports (terminal planes) far from the reference planes surrounding the discontinuity, calculating the values of capacitances and inductances of the

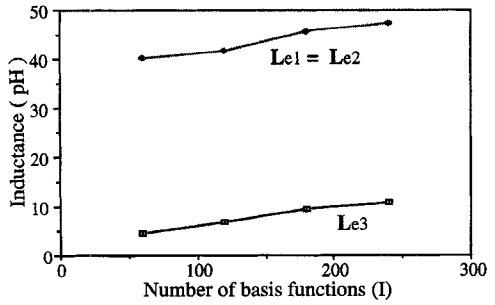

Fig. 3. Converge of equivalent inductances of a CPW T-junction with identical arms.

structure between the ports, and finally subtracting these values from the capacitances and inductances of the lines between the ports and the reference planes. In this process, the air-bridges are assumed to be removed from the junction, but their effects are added to the equivalent circuit as shunt capacitors.

In the technique presented, the effects of dispersion, metallization thickness, power leakage, and mode conversion are assumed negligible around the discontinuity. However, as reported in [1], [8], and [9], these assumptions should be treated carefully as they are only valid up to a certain frequency, depending on the dimensions of the CPW structure.

B. Computation of the Equivalent Capacitance

Since the quasi-static field is assumed around the junction, electrostatic problems are involved in the evaluation of the equivalent capacitance of the junction. Electric and magnetic walls as shown in Fig. 2(a) are set up around the region bounded to the reference planes. These walls should be far from the reference planes so that their effects on the capacitance of the junction can be considered negligible. The presence of the walls facilitates the solution of the Laplace equation $\Delta\varphi = 0$ where φ is the electrostatic potential function within the box. The existence of the magnetic walls at the three ports does not cause any perturbation in the electric field of the CPW lines.

Assuming the strips are at $\varphi_0 = 1$ V and the ground planes at $\varphi_0 = 0$ V, the boundary value problem in Fig. 2(a) and (b) can be solved using the spectral domain technique [10], [11]. The solution leads to a relation between charge distribution σ at the metallization and electric potential distribution φ_s at the slots

$$\mathcal{G}(\alpha_m, \beta_n)\tilde{\sigma}(\alpha_m, \beta_n) = \tilde{\varphi}_0(\alpha_m, \beta_n) + \tilde{\varphi}_s(\alpha_m, \beta_n) \tag{1}$$

In (1), tilda ($\tilde{}$) represents a two-dimensional finite Fourier transform defined as follows:

$$\tilde{f}(\alpha_m, \beta_n) = \frac{\binom{4}{2}}{ab} \int_0^a \int_0^b f(x, y) \cos(\alpha_m x) \cdot \cos(\beta_n z)\, dx\, dz \quad \binom{n \neq 0}{n = 0}$$

$$f(x, y) = \sum_n \sum_m \tilde{f}(\alpha_m, \beta_n) \cos(\alpha_m x) \cos(\beta_n z) \tag{2}$$

where $\alpha_m = (m - 1/2)\pi/a$, $m = 1, 2, \cdots$ and $\alpha_n = n\pi/a$, $n = 0, 1, \cdots$ and $\mathcal{G}(\alpha_m, \beta_n)$ is the spectral domain Green's function of the problem given by

$$\mathcal{G}(\alpha_m, \beta_n) = \{\gamma_{mn}[\varepsilon_2 \coth(\gamma_{mn}h) + \varepsilon_1 \coth(\gamma_{mn}d)]\}^{-1},$$
$$\gamma_{mn}^2 = \alpha_m^2 + \beta_n^2. \tag{3}$$

Equation (1) in which $\tilde{\sigma}$ and $\tilde{\varphi}_s$ are unknown and $\tilde{\varphi}_0$ is the transformed form of the known potentials in Fig. 2(b), can be solved using a method of moments. The one adopted here is the Galerkin method which leads to a symmetric matrix. To solve (1), the charge distribution σ over the metallization has been expanded in terms of top-hat basis functions, Fig. 2(c)

$$\sigma = \sum_{i=1}^{I} a_i \sigma_i$$

where

$$\sigma_i = \begin{cases} 1 & \text{for } \begin{cases} x_i - \Delta x_i/2 < x < x_i + \Delta x_i/2 \\ z_i - \Delta z_i/2 < z < z_i + \Delta z_i/2 \end{cases} \\ 0 & \text{otherwise} \end{cases}. \tag{4}$$

Substituting the Fourier transform of (4) in (1) and applying the Galerkin technique to the resulting equation lead to a set of linear equations from which a_i can be determined. In the application of the Galerkin method to (1), the inner product is defined as

$$\langle \tilde{f}(\alpha_m, \beta_n), \tilde{g}(\alpha_m, \beta_n) \rangle = \sum_n \sum_m \tilde{f}(\alpha_m, \beta_n)\tilde{g}(\alpha_m, \beta_n) = \frac{\binom{4}{2}}{ab} \int_0^b \int_0^a f(x, y) g(x, y)\, dx\, dy \quad \binom{n \neq 0}{n = 0}. \tag{5}$$

In the process of applying the inner product, φ_s is eliminated. This is because φ_s and σ_i are orthogonal over the interface containing the metallization.

Determination of a_i leads to the evaluation of charges on the strips and hence to the total capacitance, $C_T = \sum_{i=1}^{I} a_i$, bounded to the ports. Thus, the equivalent capacitance (C_e) of the junction can be calculated using $C_e = C_T - (l_1C_1 + l_2C_2 + l_3C_3)$ where C_p is the capacitance per unit length of the CPW at port p (p = 1, 2, 3) and l_p is the length from port p to the reference plane $r_p r_p'$, Fig. 2(b).

The technique used to compute C_T can be employed to calculate C_p in which case a one-dimensional Fourier transform together with one-dimensional top-hat functions will be involved in the solution. Details of the quasi-TEM solution of a planar line are given in [10], [11].

C. Computation of Equivalent Inductances

To evaluate the equivalent inductances of the junction, the strategy used in the previous section is followed. It is assumed that currents on the metallization give rise to magnetic field $\mathbf{H}$ in the box. Under the quasi-TEM approximation, $\mathbf{H}$ is related to a scalar magnetic potential function ψ through $\mathbf{H} = \nabla\psi$. This potential satisfies the Laplace equation, $\Delta\psi = 0$. Since currents are assumed on the metallization, the electrical properties of the side walls of the box is the reverse of those in the electrostatic case so that they do not affect the magnetic field of the CPW's at the ports, Fig. 2(a).

In order to simplify the solution of the problem, it is assumed that the top and bottom walls are at the same distance from the metallization interface. This assumption does not cause a noticeable error in the determination of the equivalent inductances. In fact, in practice the slots are usually much smaller than the substrate thickness and the field is essentially trapped around the slots. Since the dielectric does not affect the magnetic field, the consequence of the assumption appears favorably as $H_z = H_x = \partial\psi/\partial z = \partial\psi/\partial x = 0$ within the slots, leading to the fact that ψ is constant at the slots.

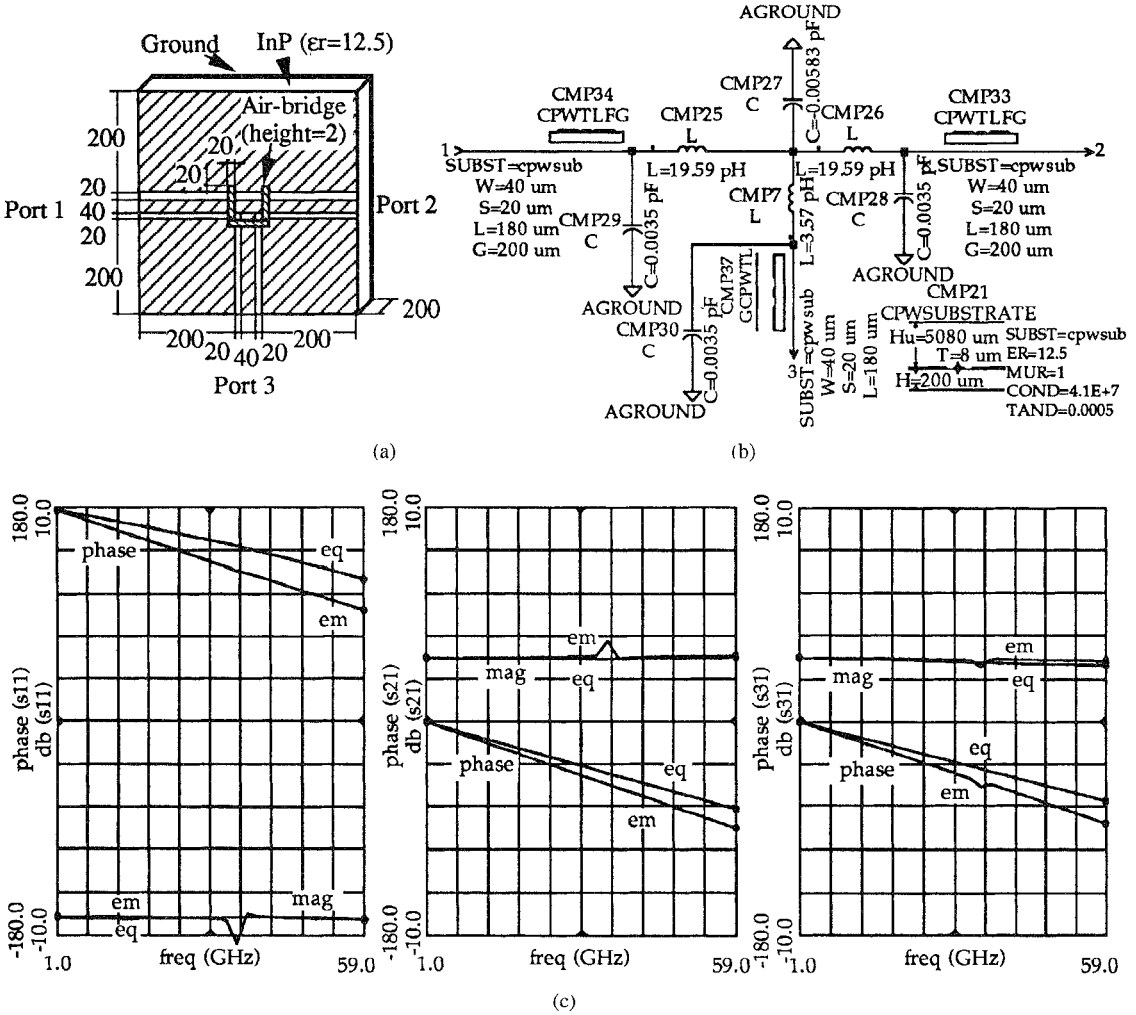

Fig. 4. Comparison of the s-parameters of a T-junction obtained by the equivalent network (eq) with those obtained by an electromagnetic simulator (em). (a) the junction (dimensions in μm), (b) the equivalent circuit, and (c) the results.

This can be exploited by assigning constant potentials to the slots in order to find the corresponding magnetic field from which other parameters such as flux, current etc., can be computed. The boundary value problem to be solved is specified within brackets in Fig. 2(a) and (b).

Using the spectral domain technique, the Laplace equation for ψ in Fig. 2(a) and (b) can be reduced to a Fourier domain relation at the air-dielectric interface

$$\mathcal{H}(\alpha_m, \beta_n)\tilde{\xi}(\alpha_m, \beta_n) = \tilde{\psi}_0(\alpha_m, \beta_n) + \tilde{\psi}_s(\alpha_m, \beta_n). \quad (6)$$

In (6), $\tilde{\psi}_0$ denotes the Fourier transform of the constant potentials ψ_{0j} (j = 1, 2, 3) at the slots, $\tilde{\psi}_s$ is the Fourier domain magnetic potential at the metallization, $\tilde{\xi}$ is the Fourier domain magnetic field normal to the interface ($\xi = H_y$ at $y = d$) and $\mathcal{H}(\alpha_m, \beta_n)$ is the spectral domain Green's function of the problem given by

$$\mathcal{H}(\alpha_m, \beta_n) = -\frac{\coth \gamma_{mn} d}{\gamma_{mn}}, \quad \gamma_{mn}^2 = \alpha_m^2 + \beta_n^2. \quad (7)$$

For an ac operation, ξ = 0 at the metallization and hence ξ and ψ_s are orthogonal in view of the inner product defined by (5).

To solve (6), the moment method has been used. The function expanded is ξ [i.e., $\xi = \sum_{i=1}^{I} b_i \xi_i$ where ξ_i is a top-hat function defined as σ_i in (4), Fig. 2(c)] which is nonzero over the slots only. Like the electrostatic case, due to the orthogonality of the basis functions (ξ_i) and ψ_s, their inner product is zero and hence the unknown potential ψ_s does not appear in the system of equations. Computing b_i from the system of equations, the normal magnetic field (ξ) at the slots is determined. This field can be used to find the magnetic flux through a slot

$$\Phi_j = \mu_0 \iint_{S_j} \xi \, ds \quad (8)$$

where $S_j (j = 1, 2, 3)$ is the surface area of the jth slot.

The inductance between any two ports can be obtained by isolating the third port [2], [3]. This condition can be simulated by assigning appropriate magnetic potentials to slots. For example, if $\psi_{01} = 1$, $\psi_{02} = -1$, and $\psi_{03} = -1$, then the current flows between ports 1 and 3 only. Thus, inductance L_{13} between these ports is given by $L_{13} = \Phi_1/4$ where 4 is the value of current at port 1 (or port 3):

$$\begin{aligned} I_1 &= I_3 \\ &= \oint \mathbf{H} \bullet d\mathbf{l} \\ &= 2 \int_{\substack{\text{stripwidth} \\ (\text{port1})}} \frac{\partial \psi}{\partial x} \, dx \\ &= 2 \int_{\substack{\text{stripwidth} \\ (\text{port3})}} \frac{\partial \psi}{\partial z} \, dz \\ &= 2 \int_{-1}^{1} d\psi \\ &= 4. \end{aligned} \quad (9)$$

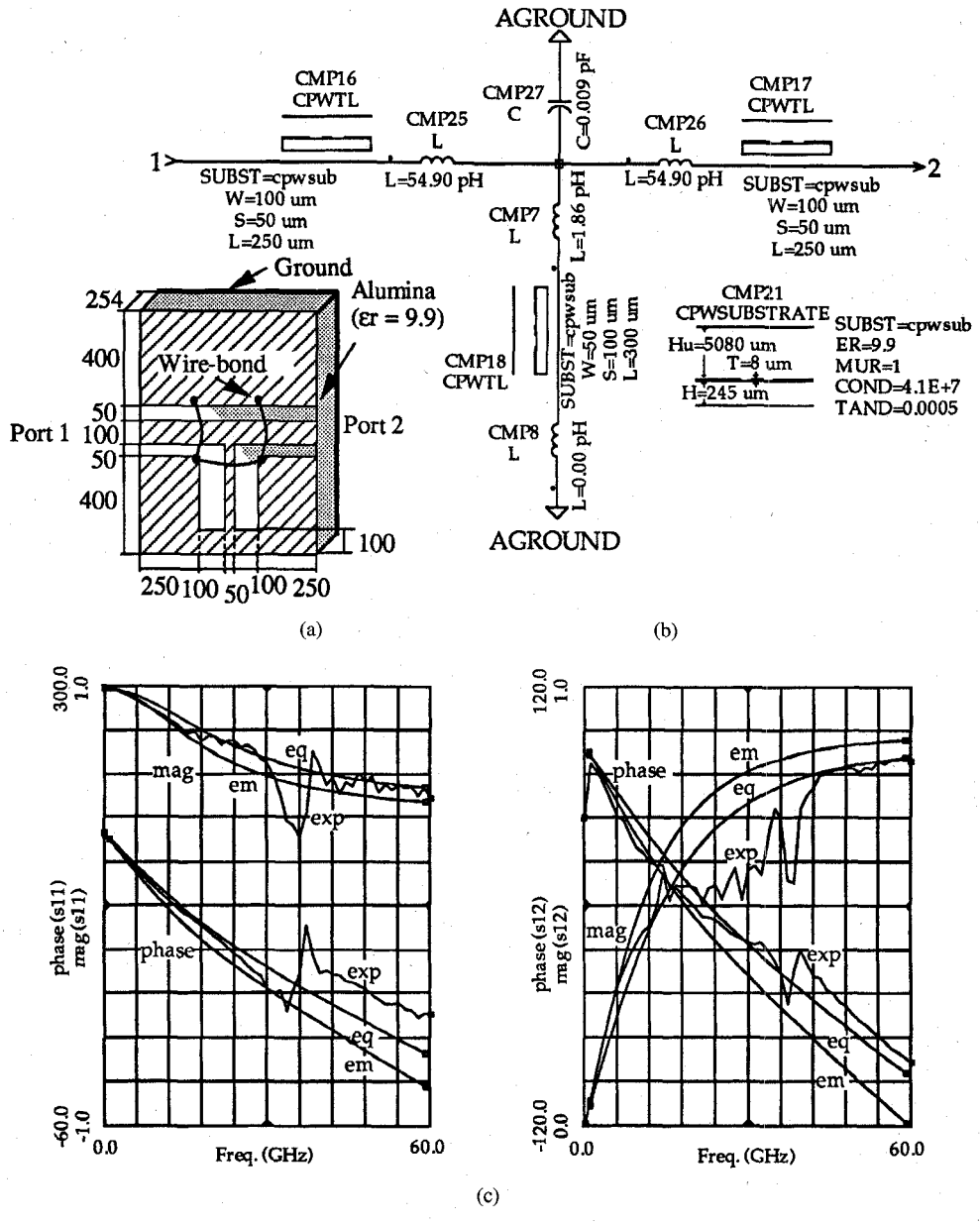

Fig. 5. S-parameters of a T-junction shorted at one port obtained by the equivalent network (eq), by an electromagnetic simulator (em), and by the measurement (exp); (a) the structure (dimensions in μm), (b) the equivalent circuit, and (c) the results.

Therefore, the equivalent inductance between planes r_1r_1' and r_3r_3' [$L_{e1} + L_{e3}$, Fig. 1(b)] is given by $L_{e1} + L_{e3} = L_{13} - l_1L_1 - l_3L_2$ where L_p is the inductance per unit length of the CPW's at port p (p = 1, 2, 3). Two other equations for inductances between ports 1 and 2 and ports 2 and 3 can be set up. These three equations yield the equivalent inductances of the area bounded to the reference planes. For the evaluation of L_1, L_2, and L_3, the Laplace equation for the magnetic potential is solved for the three CPW lines connecting to the junction.

III. Results

The technique presented was initially checked for the convergence. There are three parameters M, N (the number of Fourier terms), and I (the number of basis functions) which control the values of the components computed. The convergence can be examined by increasing I while keeping M and N sufficiently large. As an example, the convergence of the equivalent inductances of a T-junction with identical arms is presented. In this junction, the substrate is GaAs (ε_r = 12.9) with 400 μm thickness, metallized at the backside. Slots and strips are 50 and 76 μm wide, respectively, $l_1 = l_2 = l_3 = 350\,\mu$m, a = 2876 μm and b = 876 μm. A large "a" is chosen in order to avoid interference of the magnetic wall with the magnetic field of the slot. Slot 3 is discretized into 20 equal subsections in length, slots 1 and 2 each into 10 equal subsections along the length in the z-direction up to the reference planes and into another 10 equal subsections along the length in the x-direction up to the center strip. All slots are divided into K equal subsections in widths. Therefore, the number of basis functions is $I = 60K$. While maintaining $M = N = 900$, by increasing K, the number of basis functions was increased and the inductances were computed. The results are shown in Fig. 3. The final values agree with L_{e1} = 52 pH, L_{e2} = 51 pH, and L_{e3} = 6.9 pH in Table III of [4], given for a similar T-junction. Some discrepancies between the two sets of results would be due to a large underneath airbridge in the structure in [4].

To check the accuracy of the technique, the element values of the equivalent circuit of an equal-arm T-junction, Fig. 4(a), were

computed. The results are $L_{e1} = L_{e2} = 19.59$ pH, $L_{e3} = 3.57$ pH and $C_e = -5.83$ fF. The equivalent circuit was then embedded in a transmission line network, Fig. 4(b), including the air-bridge capacitances ($C = 3.5$ fF, calculated using the parallel-plate capacitor approximation) and the lengths of the CPW's from the air-bridges up to the ports defined in Fig. 4(a). Using the MDS software [12], scattering parameters s_{11}, s_{21}, and s_{31} of the network were obtained and compared against those computed by a full-wave electromagnetic simulator [5], Fig. 4(c). For the magnitudes of the scattering parameters, there is excellent agreement between the two methods. The agreement for the phases is good at low frequencies, but deteriorates as frequency increases. The maximum phase error is about 25° at 59 GHz and that has occurred for s_{11}.

The validity of the component values, $L_{e1} = L_{e2} = 54.90$ pH, $L_{e3} = 1.86$ pH, and $C_e = 9$ fF, of the equivalent circuit of a symmetrical T-junction, Fig. 5(a), computed by the present technique was supported experimentally and also confirmed theoretically using the electromagnetic simulator [5], Fig. 5(c). For the measurement, the T-junction had to be shorted at port 1. In this study, the MDS software was used to set up and analyze the equivalent transmission line network of the structure, Fig. 5(b). Some anomalies noted in the experimental results are due to energy leakage into the substrate and resonances and radiation due to long lengths of lines in the structure. In the experiment, the junction was wire-bonded at the reference planes in order to reduce the slot mode effect and as a result, uncertainties arose with the values of the capacitances of these wire-bonds with respect to the center strips. Therefore, these capacitances were not taken into account. However, this should not give rise to a significant error in the results, since the wire-bonds are not close to the metallization and hence should have negligible capacitances. Also, a perfect short circuit was considered for the shorted arm.

IV. Conclusion

A computer technique based on the quasi-static approximation for the determination of the component values of the equivalent circuits of a broad-class of CPW discontinuities was introduced. The technique enjoys the spectral domain formulation in conjunction with the method of moments for approximating the charge distributions at the conductors and the normal component of the magnetic field distribution at the slots. These distributions are used to compute the equivalent capacitances and inductances. The concepts behind the method were illustrated using an example, the CPW T-junction. The convergence of the technique for a T-junction was reported and the equivalent circuit of two other T-junctions were presented. Both the measurements and full-wave electromagnetic simulations supported the accuracy of the results.

References

[1] M. Y. Frankel, S. Gupta, J. A. Valdmanis, and G. A. Mourou, "Terahertz attenuation and dispersion characteristics of coplanar lines," *IEEE Trans. Microwave Theory Tech.*, vol. 39, pp. 910–915, June 1991.

[2] M. Naghed and I. Wolff, "Equivalent capacitances of coplanar waveguide discontinuities and interdigitated capacitors using a three-dimensional finite difference method," *IEEE Trans. Microwave Theory Tech.*, vol. 38, pp. 1808–1815, Dec. 1990.

[3] M. Naghed, M. Rittweger, and I. Wolff, "A new method for the calculation of the equivalent inductances of coplanar waveguide discontinuities," in *IEEE MTT-S Dig.*, 1991, pp. 747–750.

[4] M. Abdo-Tuko, M. Naghed, and I. Wolff, "Novel 18/36 GHz MMIC GaAs FET frequency doublers in CPW-techniques under the consideration of the effects of coplanar discontinuity," *IEEE Trans. Microwave Theory Tech.*, vol. 41, pp. 1307–1315, Aug. 1993.

[5] Sonnet Software Inc., 101 Old Cove Rd., Suite 100, Liverpool, NY 13090.

[6] P. Silvester and P. Benedek, "Equivalent capacitances of microstrip open circuits," *IEEE Trans. Microwave Theory Tech.*, vol. MTT-20, pp. 511–516, Aug. 1972.

[7] A. F. Thomson and A. Gopinath, "Calculation of microstrip discontinuity inductances," *IEEE Trans. Microwave Theory Tech*, vol MTT-23, pp 648–660, Aug. 1975.

[8] M. Riaziat, R. Majidi-Ahy, and I Feng, "Propagation modes and dispersion characteristics of coplanar-waveguides," *IEEE Trans. Microwave Theory Tech*, vol. 38, pp. 245–250, Mar 1990.

[9] W. P. Harokopus and P. B. Katehi, "Radiation loss from open coplanar waveguide discontinuities," in *IEEE MMT-S Dig.*, 1991, pp. 743–746.

[10] D. Mirshekar-Syahkal, *Spectral Domain Method for Microwave Integrated Circuits*. New York: Wiley, 1991.

[11] T. Itoh and A. S. Herbert, "A generalized spectral domain analysis for coupled suspended microstrip lines with tuning septums," *IEEE Trans. Microwave Theory Tech.*, vol. MTT-26, pp. 820–826, Oct. 1978.

[12] Hewlett-Packard Ltd., Cain Rd., Bracknell, Berkshire RG12 1HN, U.K.

High-Power HTS Planar Filters with Novel Back-Side Coupling

Zhi-Yuan Shen, Charles Wilker, Philip Pang, and Charles Carter, III

***Abstract*—Novel back-side coupling was used to produce high-power high temperature superconducting (HTS) filters. Several 2.88 GHz, 0.7% equal-ripple bandwidth, 2-pole TE_{01} mode filters were fabricated using $Tl_2Ba_2CaCu_2O_8$ HTS thin films on 20-mil $LaAlO_3$ substrates. The calibrated, measured performance of the filter at 77 K was <0.1 dB in-band insertion loss and 0.2 dB ripple up to 8 W. The uncalibrated measured performance of the filter was unchanged up to 21 W. This represents a significant advance in the power handling of planar HTS filters. These high-power, high-performance, compact HTS filters were designed to be used in transmitters for satellite communications.**

I. Introduction

High temperature superconducting (HTS) planar filters with excellent microwave performance have been demonstrated at low power [1]. The superior electrical properties of HTS materials are only realized when the current density within the HTS is less than the critical value. The power handling of any HTS filter is thus limited by the peak current and can be improved by either increasing the power handling of HTS materials [2] or by modifying the design to reduce the peak current. Recent progress in increasing the power handling has been made with the use of novel filter structures [3]–[6]. However, if HTS filters are to be used in transmitters, further improvements in power handling will be required. For example, a 1–2% bandwidth multipole filter in a satellite transmitter would be required to handle from 10 W to as much as 100 W. A compact, high-performance HTS filter operating at a temperature of 77 K or above could greatly reduce the size and weight of a transmitter. We report herein a 2.88 GHz, 0.7% equal-ripple bandwidth, two-pole TE_{01} mode HTS planar filter

Manuscript received October 17, 1995; revised February 15, 1996. This work was supported in part by Technology Reinvestment Program NASA Cooperative Agreement NCC 3-344.

The authors are with DuPont, Experimental Station, E304/C114, Wilmington, DE 19880-0304 USA.

Publisher Item Identifier S 0018-9480(96)03782-9.